Materials Science-Poland, Vol. 23, No. 2, 2005

Atomic configurations of breaking nanocontacts of aluminium and nickel

P. GARCÍA-MOCHALES[1*], P.A. SERENA[1], C. GUERRERO[2], E. MEDINA[2], A. HASMY[2]

[1]Instituto de Ciencia de Materiales de Madrid, Consejo Superior de Investigaciones Científicas, Cantoblanco, E-28049-Madrid, Spain

[2]Centro de Física, IVIC, Apdo. 21827, Caracas 1020A, Venezuela

A statistical study of favourable atomic configurations of aluminium and nickel nanocontacts during their fracture at 4 K and 300 K was performed. Nanowire breaking events are simulated by using molecular dynamics (MD), the atomic interactions being represented by the state-of-the-art embedded atom method (EAM) interatomic potentials, which are able to fit bulk and surface properties with a high degree of accuracy. A complete determination of atomic positions during the contact allows evaluation of the evolution of the minimum-cross section S_m during stretching. By accumulating S_m traces, obtained from many independent fractures of nanowires, minimum cross-section histograms $H(S_m)$ were built. These simulated histograms reveal the presence of preferential geometrical arrangements during the breaking of the nanocontact and allow a direct comparison with experimental conductance histograms. In particular, aluminium histograms show a remarkable agreement between conductance and minimum cross-section peaks. However for Ni, the interpretation of experimental conductance peaks is more difficult due to the presence of magnetic effects and the possible presence of contaminants.

Key words: *molecular dynamic; metallic nanowires; metallic nanocontacts; conductance histograms*

1. Introduction

Metallic wires with diameters of the order of few nanometers (metallic nanowires) are key components for the future development of nanoelectronics [1]. Electron transport in metallic nanowires below room temperature (RT) is ballistic since the electron elastic mean free path is larger than the characteristic nanocontact dimensions. Furthermore, well defined quantized propagating modes appear in nanowires with diame-

*Corresponding author: e-mail: pedrog@icmm.csic.es

ters of the order of few Fermi wavelengths λ_F. At such limits, the electric conductance G is described by the Landauer formula

$$G = G_0 \sum_n^N T_n$$

where $G_0 = 2e^2/h$ is the conductance quantum, e being the electron charge and h Planck's constant, T_n is the transmission probability of the n-th mode, and N is the number of propagating modes [2].

Methods based on scanning tunnelling microscopy (STM) [3, 4] and mechanically controllable break junctions (MCBJ) [5] are widely used to form metallic nanowires, although they can be also formed between macroscopic wires in "table-top" experiments [6], using electron-beam irradiation [7] or applying electrochemical methods [8].

The electrical characterisation of a metallic nanowire is done by measuring its conductance G as a function of the nanowire elongation during its rupture. The electronic transport of a given metallic species can be characterised by means of its so-called conductance histogram $H(G)$ [9] which is built from conductance curves acquired during many independent breaking events. These conductance histograms present well defined peaks. These peaks are associated with preferred conductance values which reflect the presence of conductance quantization [10] or the existence of energetically favourable atomic arrangements [11–14]. Although an exact interpretation of conductance histograms is very difficult, since they include mechanical and electronic information, they have become a standard characterisation tool for metallic nanowires.

The behaviour of $H(G)$ is even more complex for polyvalent metals since several electronic transport channels per atom are available [15]. For instance, aluminium conductance histograms obtained at 4 K [11] and room temperature [13] show well defined peaks at conductance values close to integer values of G_0, although three channels per atom are involved in electron transport. The analysis of $H(G)$ becomes even more complex in magnetic nanowires due to the presence of a new degree of freedom, the electron spin. In particular, the structure of Ni conductance histograms is not fully understood [16–20]. At RT different conductance histograms have been obtained for Ni. Some experiments have reported the existence of a featureless conductance histogram [16] whilst others reported histograms with peaks showing a strong dependence on the applied magnetic fields as well as the temperature [17]. Finally, several experiments obtained peaks located at integer values of $G_0/2$ [18, 19]. The situation is very different at $T = 4$ K in ultra high vacuum (UHV) conditions, where conductance histograms show two well defined peaks around $1.6G_0$ and $3G_0$ which do not show any dependence on the applied magnetic field [20].

The difference between low-temperature and RT Ni conductance histograms is not well understood since, in both cases, the system is below its bulk Curie temperature ($T_c = 630$ K) and similar magnetic behaviour should be expected. A possible explanation could be related to the presence of different structural Ni nanowire configurations

as a function of the temperature. The aim of the present work is to determine the validity of this hypothesis using molecular dynamics simulations to find favourable configurations in Al and Ni nanocontacts.

2. Computational procedure

Molecular dynamics (MD) has been extensively used to study the structure of breaking metallic nanowires using different interatomic potentials [12, 13, 21–23]. From knowledge of the dynamic behaviour of the nanowire, a conductance against time curve can be derived using several approaches. However, the construction of conductance histograms needs huge computational resources. A different approach is based on the construction of histograms which are able to detect the presence of favourable atomic configurations [12, 13] and this is the approach that was followed in this case.

Atomic interactions have been described within the embedded atom method (EAM) approach, using state-of-the-art interatomic potentials able to describe high and low coordinated systems [24]. Atomic trajectories and velocities were determined using the conventional Verlet velocity algorithms. Velocity scaling procedures were imposed to perform simulations at constant temperature T. In this work, the situations at $T = 4$ K and $T = 300$ K were studied.

A typical MD simulation starts with an FCC ordered supercell with 1008 atoms consisting of a parallelepiped formed of 18 (111) layers. The lattice constant a for such an initial configuration was chosen as the experimental one ($a = 3.52$ Å for Ni and $a = 4.05$ Å for Al). The z direction (stretching direction) corresponds to the (111) direction. The simulation of a single breaking event is described in detail elsewhere [12, 13]. A MD breaking event consists of two computational stages. Firstly, a balancing stage, resulting in an optimized nanowire, and secondly, a stretching stage at constant velocity until the nanowire breaks. Within the first stage the initial bulk-like configuration relaxes for 2000 MD steps keeping periodic boundary conditions (PBC) for x, y and z directions. The time interval of a MD step is $dt = 10^{-2}$ ps. Once the bulk relaxation is completed, two supporting bilayers at the top and bottom of the supercell were defined. Atomic x and y co-ordinates within these bilayers were kept constant for the rest of the simulation. Furthermore, from this moment PBC along the x and y directions were imposed uniquely to atoms forming these bilayers. The balancing procedure ends with 3000 MD steps in order to optimise the nanowire geometry prior to stretching.

During the stretching stage, both supporting bilayers are moved in opposite directions at a constant velocity of 2 m/s (2×10^{-4} Å per MD step). The dynamical evolution of nanowire atoms is driven by interatomic EAM forces. Accurate knowledge of the atomic positions permits computation of the nanowire minimum cross-section S_m using standard procedures [22]. The stretching stage is completed when the nanowire breaks (i.e. $S_m = 0$). By accumulating the geometry evolution for hundreds of breaking

events (each providing a specific $S_m(t)$ curve), minimum cross-section histograms $H(S_m)$ can be constructed.

3. Results and discussion

Figure 1 and 2 show typical minimum cross-section versus time $S_m(t)$ curves at $T = 4$ K and $T = 300$ K for Al and Ni, respectively.

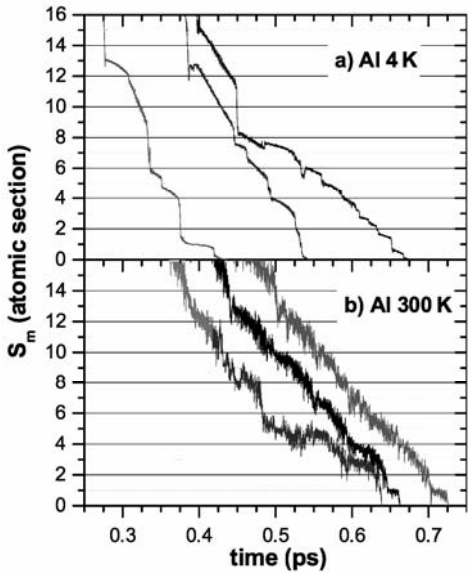

Fig. 1. Evolution of the minimum cross-section S_m (in units of atoms) as a function of time for three Al nanowires during their breaking process at: a) $T = 4$ K and b) $T = 300$ K

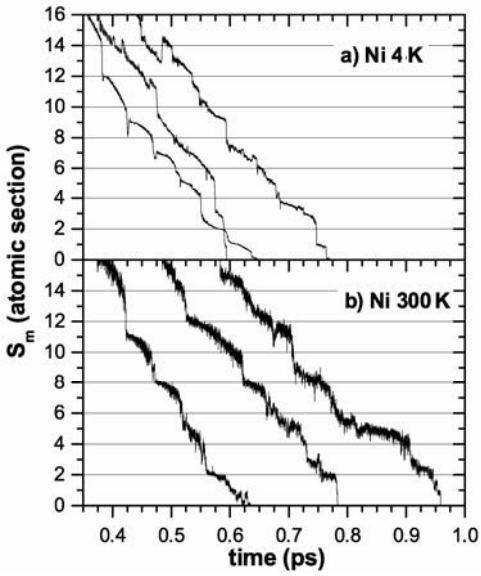

Fig. 2. Evolution of the minimum cross-section S_m (in units of atoms) as a function of time for three Ni nanowires during their breaking process at: a) $T = 4$ K and b) $T = 300$ K

The $S_m(t)$ curves show well marked jumps associated with atomic rearrangements in the nanowire. Such section jumps are correlated with jumps in the force acting on supporting slabs [21]. In general, the section steadily decreases between two subsequent jumps reflecting the existence of elastic stages during the nanowire rupture. For $T = 300$ K it can be noticed that $S_m(t)$ shows, as expected, larger fluctuations than those seen at $T = 4$ K. Minimum cross-section histograms $H(S_m)$ for Al and Ni, including 150 breaking events, are depicted in Figures 3 and 4, respectively.

Figure 4b illustrates that the statistical sampling is good since no significant differences exist between the histograms showing 50, 100 or 150 breaking events. For the low temperature ($T = 4$ K) it is clear that $H(S_m)$ presents well-defined peaks, indicating the presence of favourable atomic configurations in Al and Ni nanowires during stretching. For Al, $H(S_m)$ peak heights steadily decrease as S_m increases whereas

for Ni, certain peaks located at S_m = 5, 8, and 13 have higher a probability with respect to their neighbouring peaks. These maxima can be interpreted as precursors of ionic shell structures appearing at higher temperatures that have been observed in alkali nanowires at low temperatures [25], and Au and Al nanowires at RT [14].

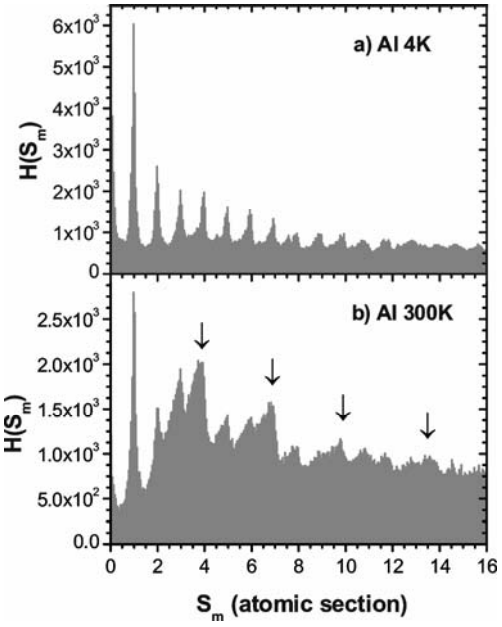

Fig. 3. Minimum cross-section histogram $H(S_m)$ obtained from 150 independent aluminium nanowire breaking events as those shown in Fig. 1 at (a) T = 4 K and (b) T = 300 K. Arrows in (b) denote those configurations with more statistical weight

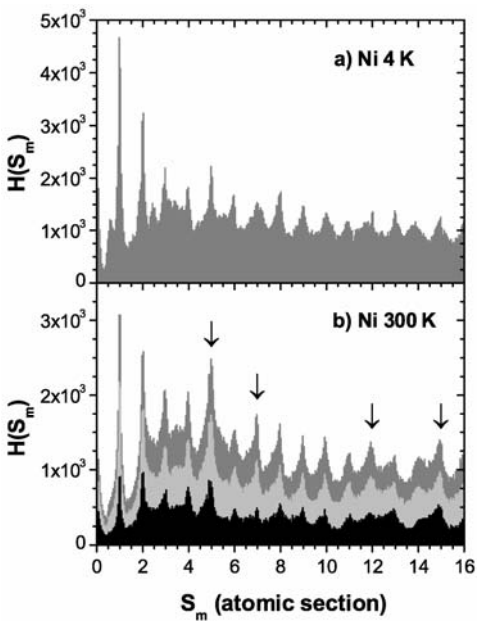

Fig. 4. Minimum cross-section histogram $H(S_m)$ obtained from 150 independent nickel nanowire breaking events as those shown in Fig. 1 at (a) T = 4 K and (b) T = 300 K. (b) shows histograms using 50 (black), 100 (light grey) and 150 (dark grey) breaking events. Arrows in (b) denote those configurations with most statistical weight

At 300 K we notice that the Al $H(S_m)$ presents a background structure, with broad peaks. The steadily decreasing sequence of local maxima is replaced by a different global shape with local maxima appearing at S_m = 1, 4, 7, 10, and 14. However, the Ni histogram at 300 K is essentially the same obtained as at T = 4 K, with small shifts in the higher probability peaks (now located at S_m = 1, 5, 7, 12, and 14). Such high-stability configurations could be interpreted as ionic magic configurations and the present set of simulations also show their existence for nickel nanocontacts. Therefore a temperature increase to 300 K strongly modifies $H(S_m)$ in the case of Al nanowires, whereas the Ni histogram keeps its main features over a wide temperature range. This difference could be explained in terms of a very different number of accessible configurations during breaking processes at RT due to the large difference between cohesion energies of Al (melting point at 960 K) and Ni (melting point at 1700 K).

4. Conclusions

It has been demonstrated that Ni configuration histograms are not dramatically affected by a temperature increase within the range of 4–300 K. However, Al histograms show a noticeable change over the same temperature range. For Al, minimum cross-sections histograms are very similar to conductance histograms at low and room temperatures. Therefore it is possible to identify, one to one, favourable geometrical configurations with favourable conductance peaks.

However, this is not true for Ni. The calculations demonstrate that in the range of 4–300 K there is a high probability peak at $S_m = 1$ which can be associated with the first conductance peak of Ni at $T = 4$ K (centred around $G = 1.6G_0$). However, there is no evidence of such a peak at room temperature in the experiments. Therefore, different structural evolutions for Ni must be excluded as the origin for experimental differences between Ni conductance histograms at low and room temperature. Such differences could be due to (i) the presence of chemiadsorbed atoms on the nanowire [20] or (ii) ballistic magnetoresistance (BMR) effects due to the presence of an abrupt magnetic domain wall anchored at the narrowest cross-section of the nanowire [26].

Acknowledgements

Thanks are expressed to J.L. Costa-Krämer and M. Díaz for helpful discussions. This work has been partially supported by the CSIC-IVIC researchers exchange programme and the Spanish DGICyT (MEC) through Projects MAT2000-0033-P4 and BFM2003-01167/FISI.

References

[1] AGRAÏT N., LEVY-YEYATI A.,VAN RUITENBEEK J.M., Phys. Rep., 377 (2003), 81 and references therein.
[2] LANDAUER R., Phil. Mag., 21 (1970), 863.
[3] PASCUAL J.I., MÉNDEZ J., GÓMEZ-HERRERO J., BARÓ A.M., GARCÍA N., BINH V.T., Phys. Rev. Lett., 71 (1993), 1852.
[4] OLESEN L., LAEGSGAARD E., STENSGAARD I., BESENBACHER F., SCHIOTZ J., STOLTZE P., JACOBSEN K.W., NORSKOV J.K., Phys. Rev. Lett., 72 (1994), 2251.
[5] MULLER C.J., VAN RUITENBEE K J.M., DE JONGH L.J., Phys. Rev. Lett., 69 (1992), 140.
[6] COSTA-KRÄMER J.L., GARCÍA N., GARCÍA-MOCHALES P., SERENA P.A., Surf. Sci., 342 (1995), L1144.
[7] KONDO Y., TAKAYANAGI K., Phys. Rev. Lett., 79 (1997), 3455; OHNISHI H., KONDO Y., TAKAYANAGI K., Nature (London), 395 (1998), 780.
[8] LI C.Z., TAO N.J., Appl. Phys. Lett., 72 (1998), 894.
[9] OLESEN L., LAEGSGAARD E., STENSGAARD I., BESENBACHER F., SCHOLTZ J., STOLTZE P., JACOBSEN K.W., NORSKOV J.K., Phys. Rev. Lett., 74 (1995), 2147.
[10] KRANS J.M., VAN RUITENBEEK J.M., FISUN V.V., YANSON I.K., DE JONGH L.J., Nature, 375 (1995), 767.
[11] YANSON A.I., VAN RUITENBEE K J.M., Phys. Rev. Lett., 79 (1997), 2157.
[12] HASMY A., MEDINA E., SERENA P.A., Phys. Rev. Lett., 86 (2001), 5574.
[13] DÍAZ M., COSTA-KRÄMER J.L., SERENA P.A., MEDINA E., HASMY A., Nanotechnol., 12 (2001), 118.

[14] MEDINA E., DÍAZ M., LEÓN N., GUERRERO C., HASMY A., SERENA P.A., COSTA-KRÄMER J.L., Phys. Rev. Lett., 91 (2003), 026802.
[15] SCHEER E., JOYEZ P., ESTEVE D., URBINA C., DEVORET M.H., Phys. Rev. Lett., 78 (1997), 3535.
[16] COSTA-KRÄMER J.L., Phys. Rev. B, 55 (1997), R4875.
[17] OSHIMA H., MIYANO K., Appl. Phys. Lett., 73 (1998), 2203.
[18] ONO T., OOKA Y., MIYAJIMA H., OTANI Y., Appl. Phys. Lett., 75 (1999), 1622.
[19] SHIMIZU M., SAITOH E., MIYAJIMA H., OTANI Y., J. Magn. Magn. Mater., 239 (2002), 243.
[20] UNTIEDT C., DEKKER D.M.T., DJUKIC D., VAN RUITENBEEK J.M., Phys. Rev. B, 69 (2004), 081401(R).
[21] LANDMAN U., LUEDTKE W.D., BURNHAM N.A., COLTON R.J., Science, 248 (1990), 454.
[22] BRATKOVSKY A.M., SUTTON A.P., TODOROV T.N., Phys. Rev. B, 52 (1995), 5036.
[23] SORENSEN R., BRANDBYGE M., JACOBSEN K.W., Phys. Rev. B, 57 (1998), 3283.
[24] MISHIN Y., FARKAS D., MEHL M.J., PAPACONSTANTOPOULOS D.A., Phys. Rev. B, 59 (1999), 3393.
[25] YANSON A.I., YANSON I.K., VAN RUITENBEEK J.M, Phys. Rev. Lett., 87 (2001), 216805.
[26] GARCÍA N., MUÑOZ M., ZHAO Y.W., Phys. Rev. Lett., 82 (1999), 2923.

Received 6 September 2004
Revised 13 January 2005